The Scientific Temper (2023) Vol. 14 (3): 826-833

E-ISSN: 2231-6396, ISSN: 0976-8653

Doi: 10.58414/SCIENTIFICTEMPER.2023.14.3.41

https://scientifictemper.com/

RESEARCH ARTICLE

Synthesis and characterization of ZnO, ZnO doped Ag_2O nanoparticles and its photocatalytic activity

V. Samuthira Pandi[1*], B. R. Senthil Kumar[2], M Anusuya[3], Annu Dagar[4]

Abstract

Zinc oxide (ZnO) has a variety of characteristics, including optical, electrical, mechanical, thermal, and structural. Nanoparticles (NPs) play a big part in many different industries. The current research focuses on producing ZnO Nps for photocatalytic dye degradation activities. Ag_2O-doped ZnO was produced together with three other different types of ZnO NPs. Nps as well as pure ZnO nanocrystals, were recovered using chemical and biological methods. The SEM study supported the chemical evolution of the ZnO nanorod-like structure, which exhibits enhanced photocatalytic activity. It was predicted that chemically produced ZnO Nps would have 34 nm, the typical particle size. X-ray diffraction analysis was used to identify Ag_2O/ZnO nanoparticles in their hexagonal configuration. The particle size ranged from 16 to 17 nm, which was shown to be the norm. The findings of the SEM study further demonstrate that the created Ag_2O doped ZnO Nps agglomerated into hexagonal forms, stuck together as bulks and rods, and grew in size in proportion to the Ag nanofluids. We conclude that hexagonal and rod-shaped Ag2O/ZnO Nps aggregates work well as photocatalytic catalysts. Approximately 25 mL of ZnO-doped Ag_2O nanofluid is a powerful photocatalyst for oxidizing organic dyes and is suitable for large-scale applications.

Keywords: TEM, Photocatalysis, Doping, Zinc oxide, Nanoparticles.

Introduction

As a result of their diverse applications in science as well as their unique characteristics, NPs have recently received a lot of attention (Alhokbany *et al*., 2022). The behavior of materials at the nanoscale, which is commonly discovered to have particularly desirable characteristics, is influenced by size confinement, the dominance of interfacial processes, and quantum effects. Zinc oxide (ZnO) is an n-type semiconductor with a significant exciton binding energy of roughly 60 meV and a large direct band gap of 3.37 eV (Chakraborty, U *et al*., 2021). This has created numerous new opportunities for numerous applications, including piezoelectric transducers, photocatalysts, and light-emitting diodes. Many scientists are now fascinated by the photocatalytic and antibacterial characteristics of ZnO particles (Rosman N *et al*., 2019). Radiation exposure causes ZnO's valence band and conduction band to produce two positive holes and electrons (Noelson E. *et al*., 2022). The positive hole and electron cause OH radicals to form as a result of their secondary interactions (Ding *et al*., 2019). Degradation of organic pollutants occurs when they interact with the potent oxidant OH radical. ZnO cannot be used as a photocatalyst under visible light due to its 3.3 eV wider band gap (Khalid *et al*., 2021).

Numerous methods, which may be further broken down into physical, biological, and chemical processes, can be used to create ZnO nanocrystals (Rosman *et al*., (2018). Chemicals, including zinc nitrate, sodium hydroxide, ammonium hydroxide, organic amines, and zinc acetate dehydrate, are often used in solution-based synthesis methods (Shume, W. M. *et al*., (2020). Scientists are hunting

[1]Centre for Advanced Wireless Integrated Technology, Chennai Institute of Technology, Chennai, Tamil Nadu, India

[2]Department of Aeronautical Engineering, Nehru Institute of Engineering And Technology, Coimbatore, Tamil Nadu, India.

[3]Department of Physics, Indra Ganesan College of Engineering, Tiruchirappalli, Tamil Nadu, India.

[4]Department of Electrical and Electronics Engineering, Maharaja Surajmal Institute of Technology, Janakpuri, New Delhi, India

***Corresponding Author:** V. Samuthira Pandi, Centre for Advanced Wireless Integrated Technology, Chennai Institute of Technology, Chennai, Tamil Nadu, India, E-Mail: samuthirapandiv@citchennai.net

How to cite this article: Pandi, V.S., Kumar, B.R.S., Anusuya, M., Dagar, A. (2023). Synthesis and characterization of ZnO, ZnO doped Ag2O nanoparticles and its photocatalytic activity. The Scientific Temper, **14**(3): 826-833.

Doi: 10.58414/SCIENTIFICTEMPER.2023.14.3.41

Source of support: Nil

Conflict of interest: None.

© *The Scientific Temper. 2023*

Received: 05/07/2023 **Accepted:** 13/08/2023 **Published** : 25/09/2023

for ZnO nanocrystals even though numerous biologically based synthetic methods are well known (Ibraheem, A. M. & Kamalakkannan, J. (2020). Biological activities are responsible for the development of an ecofriendly approach for synthesizing nanoparticles (Song *et al.*, (2021), (De, A. K. & Sinha, I. (2022). Creating silver nanoparticles using non-toxic components like plant extract and microorganisms has many benefits for medical usage (Yang *et al.*, (2018). The creation of ZnO nanostructures using the amino acid L-lysine and lemon juice has been the subject of several research (Shahzad *et al.*, (2022), (Rashmi *et al.*, (2020). Alfalfa plants have the ability to biosynthesize gold nanoparticles. Green chemistry should become more well-known when environmentally acceptable methods for producing nanoparticles are established. The effectiveness of metal-doped ZnO nanoparticles as photocatalysts has been assessed in several studies. Tb-ZnO and Sr-ZnO have both been studied for their effectiveness as photocatalysts (Rosman *et al.*, (2020), (Mohamed *et al.*, (2020). Chandekar and colleagues have used flash combustion to produce La-ZnO, which functions as an active photocatalyst (Wani, S. I. & Ganie, A. S. (2021). Similarly, other researchers have added metals including La, Mn, Bi, Fe, and Cu to ZnO to boost ZnO's photocatalytic efficiency (Peng *et al.*, (2022). Progress is being made in the study of the biological and photocatalytic properties of ZnO NPs (Xiang. & Shao, C. L. (2021). ZnO NPs and metal ion doped ZnO's photocatalytic activity were evaluated by measuring how well MB dye degraded under UV illumination (De, A. K., Majumdar, S *et al.*, (2020),(Tijani, J. O *et al.*, (2019). Additionally, ZnO NPs perform as bioactive compounds with a range of applications, such as antioxidant and antibacterial properties (Shaukat, N *et al.*, (2021), (Shen *et al.*, (2020). Uncertainty exists about Ag-doped Zno NPs' photocatalytic activity and biocompatibility. Testing was carried out in accordance with parameters including pH, [Ag+] ratios, and time periods. The presence of bioactive substances, such as polyphenols (flavonoids) that include hydroxyl groups was hypothesized to be optimally produced when silver oxide NPs were produced utilizing a plant extract-mediated synthesis method. To guarantee that free entities from the silver nanoparticles were separated from the final result, the product was centrifuged for a few minutes. This was followed by several washing with copious volumes of clean water and ethanol (Ling *et al.* (2021), (Bian *et al.*, (2020). Because OH attaches the OH group to Ag+ and promotes the synthesis of very unstable AgOH, which is quickly oxidized to Ag_2O by freeze-drying (Salari *et al.* (2018)., the presence of OH may play a role in the formation of Ag_2O NPs.

Scientists have recently focused on developing nanoscale ZnO materials to remove dyes. There are several ways to make ZnO nanoparticles, such as the sol-gel technique (Sahu, P. & Das, D. (2022), the microwave method (Liang, Y. C *et al.*, 2019), (Su, Y *et al.*, 2019), hydrothermal method (Loka C. & Lee, K. S. 2022), (Wang *et al.*, 2021)., and precipitation method (Anikina *et al.*, 2022), (Ahamad, T *et al.*,), and thermal breakdown method (Shah, A *et al.*, 2019), (Amiri *et al.*, 2020), (Adeel *et al.*, 2021). One of them is the thermal decomposition approach, which is regarded as a "green method" because it doesn't utilize or create any potentially harmful chemicals or solvents (Amani-Ghadim, A. R *et al.*, 2021). With this method, many samples may be prepared in a single batch. As a result, the current study's goal is to examine how Ag doping affects the physicochemical characteristics, ZnO NPs' ability to photocatalyze and biocompatibility. The simple sol-gel process was used to produce pure and Ag-doped (1, 2, 5, and 7.5 mol%) ZnO NPs. SEM and X-ray diffraction (XRD) analysis were used to investigate the manufactured samples. The photocatalytic activity of both pure and Ag-MgO NPs was examined using the methylene blue (MB) dye degradation.

Materials and Methods

Synthesis procedure of pure ZnO nanoparticle via chemical route

The pure ZnO NPs are made using the precipitation procedure. Figure 1 illustrates the aqueous solution that was produced using various molar ratios of $Zn(COOCH_3)2.2H_2O$ and NaOH [0.5M:0.1M, 1M:0.1M, and 1M:0.5M]. A zinc acetate aqueous solution was agitated for 20 minutes. $Zn(COOCH3)2.2H_2O$ solution was aqueously added to (Saeed, M *et al.* 2021). NaOH while it was still at room temperature, drop by drop. The mixed solutions were continuously swirling at a speed of 600 rpm for two hours. The milk-white precipitate was separated by triple centrifugation and then rinsed with deionized water after the interaction of $Zn(COOCH3)2.\ 2H_2O$ and NaOH solutions. The precipitates were rinsed, gathered, and heated to 70°C for drying. ZnO nanocrystals are made by annealing the generated particles for two hours at 400°C in a programmed furnace. The standard approach was applied for a range of molar concentrations of ZnO NPs.

Synthesis Procedure of Pure ZnO NPs through Natural Extract

Figure 2 illustrates how to boil a 500 g piece of aloe leaf in deionized water after it has been well-washed and sliced.

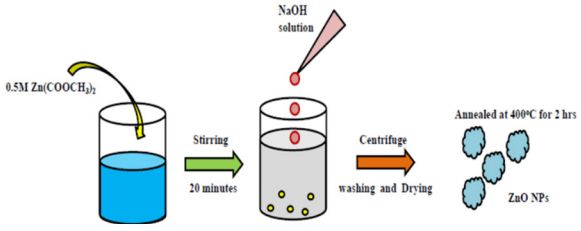

Figure 1: Synthesis procedure of pure ZnO nanoparticle

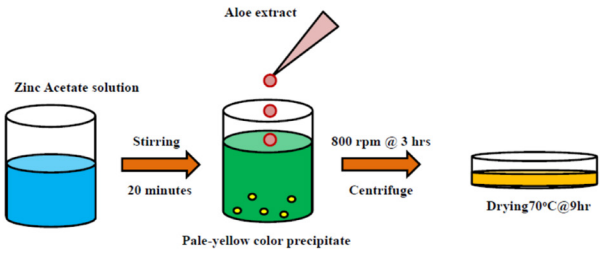

Figure 2: Synthesis of ZnO NPs from the biological route

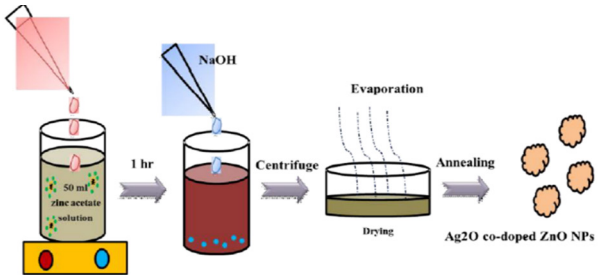

Figure 3: Synthesis procedure of ZnO doped Ag2O nanoparticle

The 500 g remaining inner gel broth from the aloe leaf was crushed and thinly pasted with just enough deionized water. For future exams, the gel paste was stored in the refrigerator. The preparation of the aloe extract and gel followed accepted procedures. The required amount of aloe extract was progressively added after agitating the Zn(COOCH3)2.2H_2O solution for 20 minutes. The mixture was constantly agitated at 800 rpm for three hours. A precipitate with a faint yellow color resulted from the reaction once it was complete. After gathering and centrifuging the precipitate, deionized water was used to clean it. With ethanol and water, the washing and centrifuging procedures were repeated. The samples were gathered, heated to 70°C in a hot air atmosphere, then dried for 8 to 9 hours.

Synthesis Procedure of ZnO Doped Ag_2O NP

Millingtonia hortensis was weighed at 10 grams, thrice washed in distilled water, and then macerated into minute pieces. Figure 3 illustrates the procedure for heating this chemical to 80°C for 30 minutes after placing it dissolved in 100 cc of distilled water in a 250 mL Erlenmeyer flask. Utilizing Whatman filters, the plant matter is then eliminated. The extract and No. 1 filter paper were combined to make silver nanoparticles. A silver nitrate ($AgNO_3$) 1 M aqueous solution was prepared in order to produce silver oxide NPs. 10 mL of the extract were added to the 1 M silver nitrate solution, and for 30 minutes, a magnetic stirrer was used to mix the solution constantly. When the reaction is done, Ag_2O NPs are produced as indicated by a change in the color of the flower extract. The extract shows color changes between 0 and 30 minutes.

At room temperature, 0.1 M Zn($COOCH_3$)2. 2H_2O was broken down in 50 cc of DD water. In order to preserve pH, the previously prepared precursor solution was added to 10 mL of Ag_2O nanofluids and continuously stirred for an hour. Then, the necessary volume of 0.1 M sodium hydroxide solution was added drop by drop while stirring continuously for an additional hour. A precipitate that was dark brown in hue was created after the stirring process. The precipitate was thoroughly washed before being dried for an hour at 800°C in a hot air oven by centrifuging it twice for 15 minutes at 4000 rpm. A two-hour, 450°C annealing operation was performed on the completed item. Ag_2O nano fluid solutions in 15, 20, and 25 mL quantities underwent the standard process. The acquired dry precursors were ground into a powder and stored for upcoming research in sealed containers (Vignesh, S *et al.*, 2021).

Characterization of Synthesized NPs

Powder X-ray diffraction (PXRD) was used to analyze the produced nanocrystals to determine their structure, crystal phase, and crystallite sizes. Analyses were performed at room temperature using CuK radiation (= 1.5406), an accelerating voltage of 40 kV, and an emission current of 30 mA. The samples' morphology and the creation of ZnO and Ag_2 doped Zno nanocrystals (JOEL JSM-6390LV) were both examined using SEM. It is determined how photocatalytically active the produced materials are using a UV-vis spectrophotometer (Bigvision 2371). Using a 12W Philips UV lamp with a peak wavelength of 354 nm, the specimens are stored in a quartz photochemical reactor (Suo, J *et al.*, 2022).

Results and Discussion

PXRD studies of chemically synthesized pure ZnO nanocrystal

Powder X-ray diffraction (PXRD) studies are used to determine the structure, crystal phase, and crystallite sizes of the generated nanocrystals. Figure 4 displays the diffraction peaks of chemically produced ZnO nanocrystals. Figure 5 illustrates how closely the ZnO wurtzite structure's (100), (002), (101), (102), (110), (103), 112, and (201) planes match the standard JCPDS No: 36–1451. These planes have peaks at 2 (degree) that are, respectively, 31.95, 34.70, 36.52, 47.78, 57.07, 63.15, 67.72, and 68.94. The estimated values for the lattice parameters, a = 3.267 and c = 5.243, are in good agreement with what is anticipated for the ZnO wurtzite structure. The lattice parameters shown in equation 1 have been calculated using the relation [(Yang, M *et al.*, (2019), formula].

1/d2 = 4/3[(h2+hk+k2/a2)]+l2/c2 ….. (1)

The computed values, a = 3.248 and c = 5.215, and the published standard values, a = 3.249 and c = 5.206 (JCPDS no. 36-1451), are in good agreement with one another. The semi-empirical Scherer's formula for calculating the average particle size (D) is shown in Equation 2.

D= k λ / β cosθ (3.2) ….. (2)

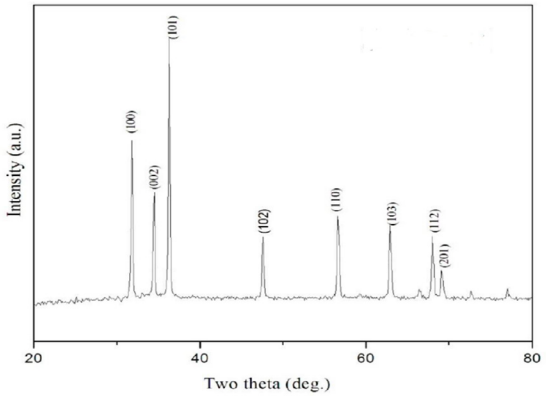

Figure 4: XRD-pattern of ZnO nanocrystals prepared by chemical method

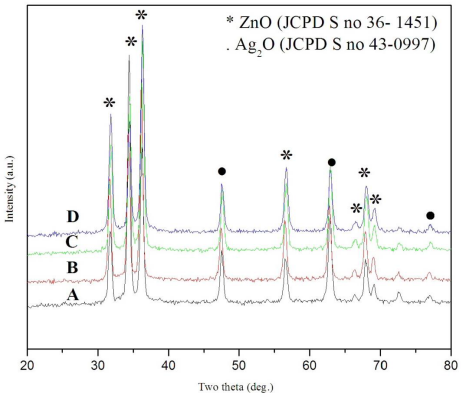

Figure 5: XRD pattern of (A)ZnO /Ag_2O(10 mL) (B)ZnO /Ag_2O(15 mL) (C)ZnO /Ag_2O(20 mL) (D)ZnO /Ag_2O(25 mL) NPs

the form factor (k), the X-ray wavelength (1.5406), the Bragg angle (degree), and the X-ray wavelength, as well as the peak position at quarter-optimum (PPQO). The PPQO value was determined using profile fitting utilizing an XRD pattern processing tool. According to chemical research, the typical crystallite size of ZnO nanocrystals is 34 nm.

PXRD studies of ZnO doped Ag_2O nanoparticle

Ag_2O diffraction peak strength increases together with the amount of Ag_2O nanofluids. However, the Ag_2O doped samples' XRD patterns exhibit a little shift to a greater angle when compared to the pure ZnO diffraction patterns, indicating that no new phases have formed. High-intensity peaks (100), (002), and (101) in Figure 6 show that the film prefers to be oriented along the c-axis. Zn and Ag have different ionic radii. Therefore, when Zn^{2+} is swapped out for Ag^{2+}, the lattice is compressed, which causes the peak to move towards high angles. Such an angle shift occurs when Ag is replaced for Zn because of a change in "d" (Liu, J *et al.*, (2022). Band gap investigations and solid solution characteristics have shown that Zn/MgO thin films made by spray pyrolysis and pulsed laser deposition (PLD) exhibit comparable behaviors (Nasab, N. K *et al.*, (2020). Additionally, using Scherer's semi-empirical approach

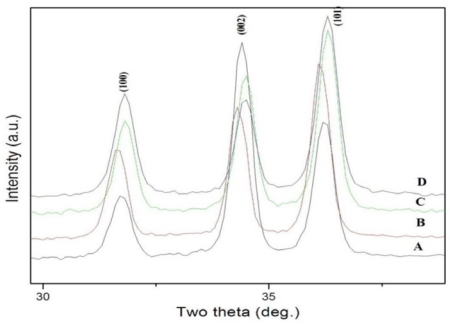

Figure 6: Shifting of XRD peaks for (A) ZnO /Ag_2O(10 mL) (B) ZnO / Ag_2O(15 mL) (C)ZnO /Ag_2O(20 mL) (D)ZnO /Ag_2O(25 mL) NPs

(Bayati F *et al.*, (2021). and parameters including the form factor of 0.94 k, the full width at half maximum (FWHM), the X-ray wavelength of 1.5406 degrees, and the Bragg angle of degrees, the average particle size (D) for various volumes of Ag_2O doped ZnO was computed. Using profile fitting and an XRD pattern processing tool, the value of FWHM was determined. For the ZnO/AgO (10 mL), ZnO/AgO (15 mL), ZnO/AgO (20 mL), and ZnO/AgO (25 mL) NPs, respectively, the average grain size (or crystalline size) was discovered to be 16, 17, 16, and 16 nm. As a result, the average crystal size of ZnO/Ag_2O NPs is 16 nm.

PXRD Studies of Naturally Synthesized Pure ZnO Nanocrystal

Natural ZnO nanocrystals were isolated, and Figure 7 shows their X-ray diffraction pattern. The sharp and precise diffraction peaks reveal the remarkable quality of the synthetic ZnO crystals. It is possible to utilize each of the XRD pattern's diffraction peaks to identify the hexagonal structure of the finely crystalline ZnO. The ZnO planes (100), (002), and 69.12 at 2 (degree) are where the diffraction peaks at 31.76, 34.43, 36.267, 47.569, 56.62, 62.88, and 69.12 are located. (101), (102), (110), (103), (112), and (201). ZnO nanocrystals' typical crystallite size was determined to be 31 nm utilizing a biological method.

Both methods produce pure ZnO nanocrystals that have the hexagonal wurtzite structure seen in their diffraction peaks. Compared to biological manufacturing, ZnO nanocrystals made chemically have sharp, straight peaks. The pattern also lacks any further peaks, indicating that all of the precursors have been completely degraded. All artificial nanocrystals have mesoporous properties.

Scanning Electron Microscope

The SEM images of ZnO nanocrystals made chemically are shown in Figure 8a. It is clear from the depiction that chemically generated ZnO nanocrystals have agglomerated hexagonal shapes and rod-like structural characteristics, as shown in Figure 8b. At concentrations of 0.5:1 M and 1:0.1 M, it is clear that the ZnO nanocrystals formed have a hexagonal structure. Nanoflakes resemble ZnO nanoparticles produced

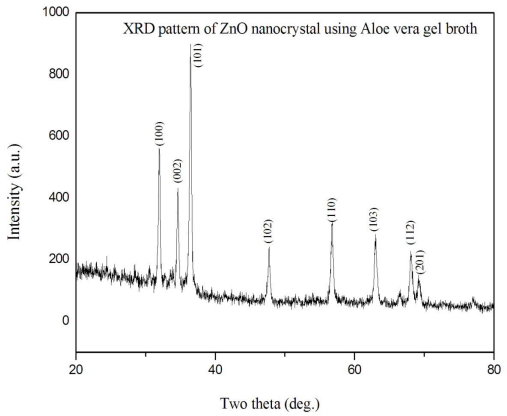

Figure 7: XRD pattern of Naturally extracted ZnO nanocrystals

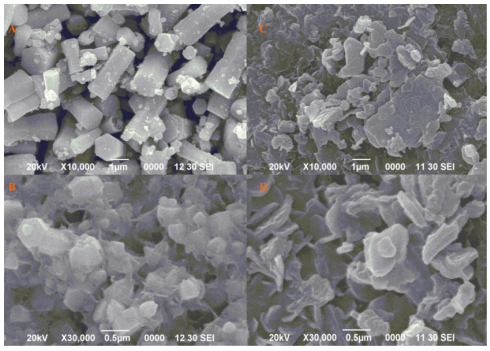

Figure 8: SEM images of (i) Chemically produced ZnO a) At 10000X b) At 30000X (ii) Naturally synthesized ZnO c) At 10000X d) At 30000X

by natural sources. The surface shapes of ZnO nanocrystals made chemically and those made organically are readily distinguished in Figure 8c. The example also shows that, in contrast to those made using chemical procedures, ZnO nanocrystals created using biological methods yield uneven bulks as seen in Figure 8d.

The produced samples were examined under a scanning electron microscope to understand more about their shape and microstructure. Figure 9 demonstrates the hexagonal morphologies and interconnected rods and bulks of the Ag_2O doped ZnO NPs. With an increase of Ag_2O nanofluids, the hexagonal forms of the rods structure expand. The fact that the nanorods are aggregated suggests that a sizable amount of doping agent (25 mL Ag_2O nanofluids) was used. The effect of mixing speed while adding the aqueous AgNP solution at high concentrations on the mean agglomeration size and repeatability has also been proven. The agglomeration rate is presumably modest at this concentration because it is easier to disperse particles that are close to the primary particle size at lower concentrations.

Photocatalytic activity of ZnO Nanorods

When the catalyst is exposed to light for long periods—1, 2, 3, and 4 hours—the curves' initial slopes of the absorption rate noticeably rise. This is seen in Figure 10. It indisputably proves that the 1:0.1 M concentration produces higher

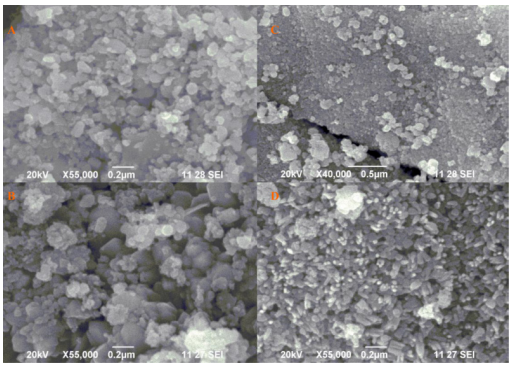

Figure 9: SEM images of (a) ZnO /Ag_2O(10 mL) ;(b) ZnO /Ag_2O (15 mL); (c) ZnO /Ag_2O (20 mL);(d) ZnO /Ag_2O (25 mL) NPs

photocatalytic activity when all molar concentrations of ZnO nanorods manufactured using the chemical technique are compared (Yu, H. L *et al.*, (2020). The more time that passed, the lower the MB dye concentration was. The effectiveness of photodegradation at 1:0.1 concentrations after 4 hours of exposure is 76%. Their enhanced catalytic activity is due to the nanorods' larger surface area when compared to other structures. Ag to ZnO undergoes a photoinduced electron transfer as a result of the Ag nanoparticles' conduction band electrons being pushed to the state of surface plasmon resonances. The electrons subsequently enter the ZnO conduction band after becoming more energetic. While the ZnO conduction band cannot receive electrons, the Fermi state of Ag nanoparticles can. The Fermi state electrons of the Ag nanoparticles may travel to the defect levels of ZnO, depending on the energy levels of the various ZnO defects. By employing these techniques, electron transport in fresh Ag/ZnO might be reduced to a minimum. Over a prolonged length of time, silver oxidation makes electron transport more challenging.

The resulting compounds hastened the breakdown of the Methylene Blue (MB) dye (Sabouri *et al.*, (2022). For an hour in the dark, the dye and catalyst molecules were continuously combined to come about equilibrium for adsorption and desorption. Every 15 minutes, a spectrophotometer was used to check the adsorption until it was almost constant because a photocatalytic system's photosensitizer is a constant component. In the dark, a photosensitizer often becomes unstable. The UV-visible absorption spectra of the ZnO/Ag_2O nanoparticles used to remove the MB dye are shown in Figure 11 in (a-c), and (d) formats. The wavelengths of the Ag_2O/ZnO NPs were determined to be 291, 291, and 300 nm in the volumes of 15, 20, and 25 mL, respectively. The MB dye's biggest peak in absorbance strength could be noticed at 665 nm. More Ag_2O nanofluid was added, progressively decreasing the intensity peak of the NPs that were created (Goktas A *et al.*, (2022). Here, the principal MB dye absorption peak is designated by C, while C0 stands for the absorption of the original dye solution. Degradation of several photocatalysts' efficiency

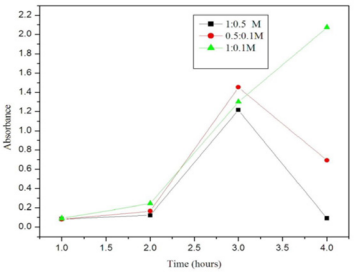

Figure 10: Photocatalytic activity of ZnO nanorods

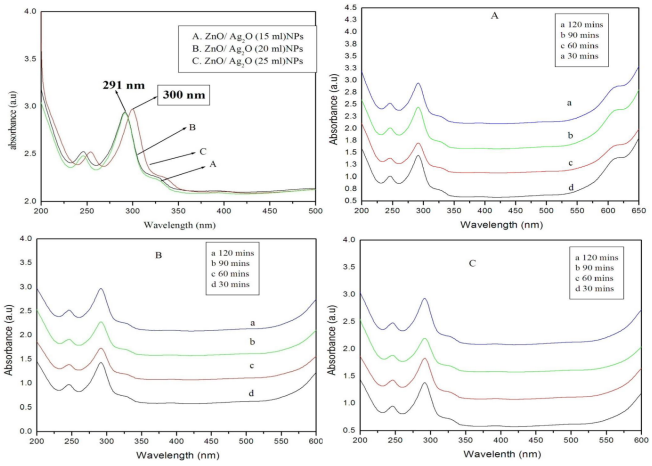

Figure 11: UV-vis spectrum of ZnO/Ag2O NPs

as a function of exposure duration (A, B, C). ZnO/Ag_2O (15 and 20 mL) NPs degrade 56% more effectively than control samples. After 120 minutes of exposure, it is interesting that ZnO/Ag_2O (25 mL) NPs have a 63% disintegration efficiency (Zelekew, O. A *et al.*, (2021). As a result, this element's function as a photocatalyst makes the breakdown of organic dyes easier for large-scale applications. A valence band electron is excited by each individual photon.

A positive hole is left in the VB after the transmission of from the conduction band (CB) to VB. This might occur due to the way the semiconductor material's and transition metal oxide's electronic band structures are set up (Zoha *et al.*, (2020). Furthermore, the breakdown of dye is brought on by hydroxyl radicals generated by electron-hole recombination. As seen below, the MB dye breaks down in the resulting Ag2O/ZnO nanoparticles. ZnO/Ag2O NPs (25 mL) act, in contrast to other nanoparticles of various sizes, as a possible catalyst for the degradation of the organic pollutant of MB dye. The maximum absorbance value dropped during a given time period, indicating the degradation of the MB dye. ZnO/Ag_2O NPs (25 mL) exhibit a greater photocatalytic activity according to the photocatalytic activity (Kamarajan *et al.*, (2022). This could be due to the synthesized NPs' higher surface areas, which also contributed to the formation of the rod-like structure and the higher volume of the green Ag_2O nanofluids. The dye may lose part of its color as a result of interactions with OH radicals or intermediate photo reactions. The size and composition of the produced metal oxide nanoparticles also influenced the rate of dye breakdown.

Conclusion

- Pure ZnO nanocrystals were produced using the chemical precipitation technique. ZnO nanocrystals were synthesized with a hexagonal structure, which was discovered using X-ray diffraction (XRD) study, and SEM analysis served as confirmation. The nanoscale zinc oxide particle's average particle sizes for nanorods and nanoflakes were 31 nm and 34 nm, respectively, clearly illustrating the poly discrepancy.
- 1:0.1 molecular concentration Compared to ZnO nanoflakes made chemically and ZnO nanoflakes at various concentrations, ZnO nanorods had a greater capacity for the degradation of MB dye by photocatalysis. The production of nanorods during chemical synthesis results in higher photocatalytic activity than nanoflakes. The greater surface area of nanorods compared to other forms may be the reason for their improved catalytic activity.
- According to an XRD analysis, the generated ZnO/Ag_2O NPs had an average crystalline size of 16 nm. The results of the SEM investigation demonstrate the hexagonal forms of the produced Ag_2O doped ZnO nanoparticles, which have gathered and are sticking as bulks and rods.
- As the Ag_2O nanofluid concentration rises, the hexagonal shapes of the rods' structure also do. UV-visible spectrum analysis of the photocatalytic investigation reveals containing 25 mL of ZnO-doped Ag_2O nanofluid efficiently (63%) and quickly (approximately 120 minutes) destroyed MB dye. As a result, the ZnO/Ag_2O NPs component under research may be used extensively as a potential photocatalytic degrader of organic dyes.

Availability of Data and Materials

The data supporting the findings of the article is available within the article.

References

Adeel, M., Saeed, M., Khan, I., Muneer, M., & Akram, N. (2021). Synthesis and characterization of Co–ZnO and evaluation of its photocatalytic activity for photodegradation of methyl orange. ACS omega, v. 6, n. 2, pp. 1426-1435.

Ahamad, T., Alhokbany, N., & Alshehri, S. M. Fabrication of Highly Porous Zno/Ag2o Nanoparticles Embedded in N-Doped Graphitic Carbon Forphotocatalytic Degradation of Tetracycline.

Alhokbany, N., Ahamad, T., & Alshehri, S. M. (2022). Fabrication of highly porous ZnO/Ag2O nanoparticles embedded in N-doped graphitic carbon for photocatalytic degradation of tetracycline. Journal of Environmental Chemical Engineering, v. 10. n. 3, pp. 107681.

Amani-Ghadim, A. R., Tarighati Sareshkeh, A., Nozad Ashan,

N., Mohseni-Zonouz, H., Seyed Ahmadian, S. M., Seyed Dorraji, M. S., ... & Bayat, F. (2021). Photocatalytic activity enhancement of carbon-doped g-C3N4 by synthesis of nanocomposite with Ag2O and α-Fe2O3. Journal of the Chinese Chemical Society, v. 68, n. 11, pp. 2118-2131.

Amiri, M., Dashtian, K., Ghaedi, M., & Mosleh, S. (2020). A dual surface inorganic molecularly imprinted Bi2WO6-CuO/Ag2O heterostructure with enhanced activity-selectivity towards the photocatalytic degradation of target contaminantst. Photochemical & Photobiological Sciences, v. 19, n. 7, pp. 943-955.

Anikina, M. A., Maximov, A. I., Gagarina, A. Y., & Kirillova, S. A. (2022, January). Synthesis Peculiarities of Photocatalytic Materials Based on Zinc Oxide. In 2022 Conference of Russian Young Researchers in Electrical and Electronic Engineering (ElConRus) (pp. 1006-1009). IEEE.

Bayati, F., Mohammadi, M. K., Yengejeh, R. J., & Babaei, A. A. (2021). Ag2O/GO/TiO2 composite nanoparticles: synthesis, characterization, and optical studies. Journal of the Australian Ceramic Society, 57, n. 1, pp. 287-293.

Bian, H., Zhang, Z., Xu, X., Gao, Y., & Wang, T. (2020). Photocatalytic activity of Ag/ZnO/AgO/TiO2 composite. Physica E: Low-dimensional Systems and Nanostructures, v. 124, pp. 114236.

Chakraborty, U., Bhanjana, G., Kaur, N., Sharma, R., Kaur, G., Kaushik, A., & Chaudhary, G. R. (2021). Microwave-assisted assembly of Ag2O-ZnO composite nanocones for electrochemical detection of 4-Nitrophenol and assessment of their photocatalytic activity towards degradation of 4-Nitrophenol and Methylene blue dye. Journal of hazardous materials, v. 416, pp. 125771.

De, A. K., & Sinha, I. (2022). Synergistic effect of Ni doping and oxygen vacancies on the visible light photocatalytic properties of Ag2O nanoparticles. Journal of Physics and Chemistry of Solids, v. 167, pp. 110733.

De, A. K., Majumdar, S., Pal, S., Kumar, S., & Sinha, I. (2020). Zn doping induced band gap widening of Ag2O nanoparticles. Journal of Alloys and Compounds, v. 832, pp. 154127.

Ding, W., Zhao, L., Yan, H., Wang, X., Liu, X., Zhang, X., ... & Tang, B. (2019). Bovine serum albumin assisted synthesis of Ag/Ag2O/ZnO photocatalyst with enhanced photocatalytic activity under visible light. Colloids and Surfaces A: Physicochemical and Engineering Aspects, v. 568, pp. 131-140.

Goktas, A., Modanlı, S., Tumbul, A., & Kilic, A. (2022). Facile synthesis and characterization of ZnO, ZnO: Co, and ZnO/ZnO: Co nano rod-like homojunction thin films: Role of crystallite/grain size and microstrain in photocatalytic performance. Journal of Alloys and Compounds, v. 893, pp. 162334.

Ibraheem, A. M., & Kamalakkannan, J. (2020). Sustainable scientific advancements modified Ag2O-ZnO thin films characterization and application of photocatalytic purification of carcinogenic dye in deionizer water and contaminated sea water solutions and synthetic, natural based dye-sensitized solar cells. Materials Science for Energy Technologies, v. 3, pp. 183-192.

Kamarajan, D., Anburaj, B., Porkalai, V., Muthuvel, A., Nedunchezhian, G., & Mahendran, N. (2022). Green synthesis of ZnO nanoparticles and their photocatalyst degradation and antibacterial activity. Journal of Water and Environmental Nanotechnology, v. 7, n. 2, pp. 180-193.

Khalid, N. R., Arshad, A., Tahir, M. B., & Hussain, M. K. (2021). Fabrication of p–n heterojunction Ag2O@ Ce2O nanocomposites make enables to improve photocatalytic activity under visible light. Applied Nanoscience, v. 11, n. 1, 199-206.

Liang, Y. C., Liu, Y. C., & Hung, C. S. (2019). Sputtering control of Ag2O decoration configurations on ZnO nanorods and their surface arrangement effects on photodegradation ability toward methyl orange. Nanotechnology, v. 30, n. 49, pp. 495701.

Ling, W., Lu, W., Wang, J., Niu, G., & Zhu, D. (2021). Hydrothermal synthesis and characterization of Ag2O/CeO2 modified 3D flower-like ZnO as the N-butanol-sensing. Materials Science in Semiconductor Processing, v. 133, pp. 105937.

Liu, J., Shi, H., Sans, C., Sun, L., Yuan, X., Pan, F., & Xia, D. (2022). Insights into the photocatalytic ozonation over Ag2O-ZnO@g-C3N4 composite: Cooperative structure, degradation performance, and synergistic mechanisms. Journal of Environmental Chemical Engineering, v. 10, n. 2, pp. 107285.

Loka, C., & Lee, K. S. (2022). Enhanced Visible-Light-Driven Photocatalysis of Ag/Ag2O/ZnO Nanocomposite Heterostructures. Nanomaterials, v. 12, n. 15, pp. 2528.

Mohamed, R. M., Ismail, A. A., Kadi, M. W., Alresheedi, A. S., & Mkhalid, I. A. (2020). Facile synthesis of mesoporous Ag2O–ZnO heterojunctions for efficient promotion of visible light photodegradation of tetracycline. ACS omega, v. 5, n. 51, pp. 33269-33279.

Nasab, N. K., Sabouri, Z., Ghazal, S., & Darroudi, M. (2020). Green-based synthesis of mixed-phase silver nanoparticles as an effective photocatalyst and investigation of their antibacterial properties. Journal of Molecular Structure, v. 1203, pp. 127411.

Noelson, E. A., Anandkumar, M., Marikkannan, M., Ragavendran, V., Thorgersen, A., Sagadevan, S., ... & Mayandi, J. (2022). Excellent photocatalytic activity of Ag2O loaded ZnO/NiO nanocomposites in sun-light and their biological applications. Chemical Physics Letters, v. 796, pp. 139566.

Peng, Y., Zhou, H., Wu, Y., Ma, Z., Zhang, R., Tu, H., & Jiang, L. (2022). A new strategy to construct cellulose-chitosan films supporting Ag/Ag2O/ZnO heterostructures for high photocatalytic and antibacterial performance. Journal of Colloid and Interface Science, v. 609, pp. 188-199.

Rashmi, B. N., Harlapur, S. F., Avinash, B., Ravikumar, C. R., Nagaswarupa, H. P., Kumar, M. A., ... & Santosh, M. S. (2020). Facile green synthesis of silver oxide nanoparticles and their electrochemical, photocatalytic and biological studies. Inorganic Chemistry Communications, 111, pp. 107580.

Rosman, N., Salleh, W. N. W., Ismail, A. F., Jaafar, J., Harun, Z., Aziz, F., ... & Takashima, M. (2018). Photocatalytic degradation of phenol over visible light active ZnO/Ag2CO3/Ag2O nanocomposites heterojunction. Journal of Photochemistry and Photobiology A: Chemistry, v. 364, pp. 602-612.

Rosman, N., Salleh, W. N. W., Mohamed, M. A., Harun, Z., Ismail, A. F., & Aziz, F. (2020). Constructing a compact heterojunction structure of Ag2CO3/Ag2O in-situ intermediate phase transformation decorated on ZnO with superior photocatalytic degradation of ibuprofen. Separation and Purification Technology, v. 251, pp. 117391.

Rosman, N., Wan Salleh, W. N., Aziz, F., Ismail, A. F., Harun, Z., Bahri, S. S., & Nagai, K. (2019). Electrospun nanofibers embedding ZnO/Ag2CO3/Ag2O heterojunction photocatalyst with enhanced photocatalytic activity. Catalysts, 9, n. 7, pp. 565.

Sabouri, Z., Sabouri, S., Moghaddas, S. S. T. H., Mostafapour,

A., Gheibihayat, S. M., & Darroudi, M. (2022). Plant-based synthesis of Ag-doped ZnO/MgO nanocomposites using Caccinia macranthera extract and evaluation of their photocatalytic activity, cytotoxicity, and potential application as a novel sensor for detection of Pb2+ ions. Biomass Conversion and Biorefinery, 1-13.

Saeed, M., ul Haq, A., Muneer, M., Ahmad, A., Bokhari, T. H., & Sadiq, Q. (2021). Synthesis and characterization of Bi2O3 and Ag-Bi2O3 and evaluation of their photocatalytic activities towards photodegradation of crystal violet dye. Physica Scripta, v. 96, n. 12, pp. 125707.

Sahu, P., & Das, D. (2022). Two-Step Visible Light Photocatalytic Dye Degradation Phenomena in Ag2O-Impregnated ZnO Nanorods via Growth of Metallic Ag and Formation of ZnO/Ag0/Ag2O Heterojunction Structures. Langmuir, v. 38, n. 15, pp. 4503-4520.

Salari, H., Daliri, A., & Gholami, M. R. (2018). Graphitic carbon nitride/reduced graphene oxide/silver oxide nanostructures with enhanced photocatalytic activity in visible light. Physical Chemistry Research, v. 6, n. 4, pp. 729-740.

Shah, A., Haq, S., Rehman, W., Waseem, M., Shoukat, S., & Rehman, M. U. (2019). Photocatalytic and antibacterial activities of paeonia emodi mediated silver oxide nanoparticles. Materials Research Express, v. 6, n. 4, pp. 045045.

Shahzad, K., Hussain, S., Nazir, M. A., Jamshaid, M., ur Rehman, A., Alkorbi, A. S., ... & Alhemiary, N. A. (2022). Versatile Ag2O and ZnO nanomaterials fabricated via annealed Ag-PMOS and ZnO-PMOS: An efficient photocatalysis tool for azo dyes. Journal of Molecular Liquids, v. 356, pp. 119036.

Shaukat, N., Ahmad, Z., Munawar, K. S., & Abbas, S. M. (2021). Synthesis, Characterization, Photocatalytic and Antimicrobial Activities of Copper Doped Silver and Nickel Oxide Nanoparticles. Lahore Garrison University Journal of Life Sciences, v. 5, n. 01, pp. 1-18.

Shen, J. C., Zeng, H. Y., Chen, C. R., & Xu, S. (2020). A facile fabrication of Ag2O-Ag/ZnAl-oxides with enhanced visible-light photocatalytic performance for tetracycline degradation. Applied Clay Science, v. 185, pp. 105413.

Shume, W. M., Murthy, H. C., & Zereffa, E. A. (2020). A review on synthesis and characterization of Ag2O nanoparticles for photocatalytic applications. Journal of Chemistry, 2020.

Song, M., Qi, K., Wen, Y., Zhang, X., Yuan, Y., Xie, X., & Wang, Z. (2021). Rational design of novel three-dimensional reticulated Ag2O/ZnO Z-scheme heterojunction on Ni foam for promising practical photocatalysis. Science of The Total Environment, v. 793, pp. 148519.

Su, Y., Zhao, X., Bi, Y., & Han, X. (2019). ZnO/Ag–Ag2O microstructures for high-performance photocatalytic degradation of organic pollutants. Clean Technologies and Environmental Policy, v. 21, n. 2, pp. 367-378.

Suo, J., Jiao, K., Fang, D., Bu, H., Liu, Y., Li, F., & Ruzimuradov, O. (2022). Visible photocatalytic properties of Ag–Ag2O/ITO NWs fabricated by mechanical injection-discharge-oxidation method. v. 204, pp. 111338.

Tijani, J. O., Momoh, U. O., Salau, R. B., Bankole, M. T., Abdulkareem, A. S., & Roos, W. D. (2019). Synthesis and characterization of Ag2O/B2O3/TiO2 ternary nanocomposites for photocatalytic mineralization of local dyeing wastewater under artificial and natural sunlight irradiation. Environmental Science and Pollution Research, v. 26, n. 19, pp. 19942-19967.

Vignesh, S., Eniya, P., Srinivasan, M., Sundar, J. K., Li, H., Jayavel, S., ... & Palanivel, B. (2021). Fabrication of Ag/Ag2O incorporated graphitic carbon nitride based ZnO nanocomposite for enhanced Z-scheme photocatalytic performance of various organic pollutants and bacterial disinfection. Journal of Environmental Chemical Engineering, v. 9, n. 5, pp. 105996.

Wang, H., Sun, T., Xu, N., Zhou, Q., & Chang, L. (2021). 2D sodium titanate nanosheet encapsulated Ag2O-TiO2 pn heterojunction photocatalyst: Improving photocatalytic activity by the enhanced adsorption capacity. Ceramics International, v. 47, n. 4, pp. 4905-4913.

Wani, S. I., & Ganie, A. S. (2021). Ag2O incorporated ZnO– TiO2 nanocomposite: Ionic conductivity and photocatalytic degradation of an organic dye. Inorganic Chemistry Communications, v. 128, pp. 108567.

Xiang, D., & Shao, C. L. (2021). Ag2O/ZnO Heterostructures with Enhanced Photocatalytic Activity. In Materials Science Forum. Trans Tech Publications Ltd. v. 1035, pp. 1043-1049.

Xu, P., Wang, P., Wang, Q., Wei, R., Li, Y., Xin, Y., ... & Zhang, G. (2021). Facile synthesis of Ag2O/ZnO/rGO heterojunction with enhanced photocatalytic activity under simulated solar light: Kinetics and mechanism. Journal of Hazardous Materials, v. 403, pp. 124011.

Yang, M., Pu, Y., Wang, W., Li, J., Guo, X., Shi, R., & Shi, Y. (2019). Highly efficient Ag2O/AgNbO3 pn heterojunction photocatalysts with enhanced visible-light responsive activity. Journal of Alloys and Compounds, v. 811, pp. 151831.

Yang, Z., Deng, C., Ding, Y., Luo, H., Yin, J., Jiang, Y., ... & Jiang, Y. (2018). Eco-friendly and effective strategy to synthesize ZnO/Ag2O heterostructures and its excellent photocatalytic property under visible light. Journal of Solid State Chemistry, 268, 83-93.

Yu, H. L., Wu, Q. X., Wang, J., Liu, L. Q., Zheng, B., Zhang, C., ... & Jia, J. R. (2020). Simple fabrication of the Ag-Ag2O-TiO2 photocatalyst thin films on polyester fabrics by magnetron sputtering and its photocatalytic activity. Applied Surface Science, v. 503, pp. 144075.

Zelekew, O. A., Aragaw, S. G., Sabir, F. K., Andoshe, D. M., Duma, A. D., Kuo, D. H., ... & Aga, F. G. (2021). Green synthesis of Co-doped ZnO via the accumulation of cobalt ion onto Eichhornia crassipes plant tissue and the photocatalytic degradation efficiency under visible light. Materials Research Express, v. 8, n. 2, pp. 025010.

Zoha, S., Ahmad, M., Zaidi, S. J. A., Ashiq, M. N., Ahmad, W., Park, T. J., & Basit, M. A. (2020). ZnO-based mutable Ag2S/Ag2O multilayered architectures for organic dye degradation and inhibition of E. coli and B. subtilis. Journal of Photochemistry and Photobiology A: Chemistry, v. 394, pp. 112472.